View metadata, citation and similar papers at core.ac.uk

brought to you by CORE

provided by Archivio istituzionale della ricerca - Alma Mater Studiorum Università di Bologna

applied sciences

MDPI

Article

Multi-Imaging Investigation to Evaluate the Relationship between Serum Cystatin C and Features of Atherosclerosis in Non-ST-Segment Elevation Acute Coronary Syndrome

Nevio Taglieri [1,*], Cristina Nanni [2], Gabriele Ghetti [1], Rachele Bonfiglioli [2], Francesco Saia [1], Francesco Buia [3], Giacomo Maria Lima [2], Valeria Marco [4], Antonio Giulio Bruno [1], Francesco Prati [4,5], Stefano Fanti [2] and Claudio Rapezzi [1]

1 Polo Cardio-Toraco-Vascolare, Dipartimento di Medicina Specialistica, Diagnostica e Sperimentale, Alma Mater Studiorum Università di Bologna, 40138 Bologna, Italy; gabriele.ghetti84@gmail.com (G.G.); francescosaia@hotmail.com (F.S.); antoniogiuliobruno@gmail.com (A.G.B.); claudio.rapezzi@unibo.it (C.R.)

2 Istituto di Medicina Nucleare, Dipartimento di Medicina Specialistica, Diagnostica e Sperimentale, Alma Mater Studiorum Università di Bologna, 40138 Bologna, Italy; cristina.nanni@aosp.bo.it (C.N.); rachele.bonfiglioli@gmail.com (R.B.); giacomo.maria.lima@gmail.com (G.M.L.); s.fanti@unibo.it (S.F.)

3 Istituto di Radiologia, Dipartimento di Medicina Specialistica, Diagnostica e Sperimentale, Alma Mater Studiorum Università di Bologna, 40138 Bologna, Italy; francescobuia82@libero.it

4 CLI Foundation, 00182 Rome, Italy; valeria.marco88@gmail.com (V.M.); fprati61@gmail.com (F.P.)

5 GVM Care & Research, Ettore Sansavini Health Science Foundation, 48033 Cotignola, Italy

* Correspondence: neviotaglieri@hotmail.it; Tel.: +39-051-2144475; Fax: +39-051-6364477

Received: 21 November 2018; Accepted: 4 February 2019; Published: 15 February 2019

Abstract: Objectives: High cystatin C(CysC) levels are associated with impaired cardiovascular outcome. Whether CysC levels are independently related to the atherosclerosis burden is still controversial. Methods: We enrolled 31 non-ST-segment elevation acute coronary syndrome patients undergoing percutaneous coronary intervention. Patients were divided into 2 groups on the basis of median value of serum CysC. Using the high CysC group as a dependent variable, univariable and multivariable analyses were used to evaluate the association between CysC and three different features of atherosclerosis: 1) coronary plaque vulnerability as assessed by optical coherence tomography (OCT), 2) coronary artery calcium (CAC) by means of computed tomography scan, and 3) aortic wall metabolic activity, as assessed using ^{18}F-Fluorodeoxyglucose-positron emission tomography (^{18}F-FDG-PET). Results: After univariable and multivariable analyses, ^{18}F-FDG uptake in the descending aorta (DA) was independently associated with a low level of CysC [(Odds Ratio = 0.02; 95%CI 0.0004–0.89; p = 0.044; ^{18}F-FDG uptake measured as averaged maximum target to blood ratio); (Odds Ratio = 0.89; 95%CI 0.82–0.98, p = 0.025; ^{18}F-FDG uptake measured as number of active slices)]. No trend was found for the association between CysC and characteristics of OCT-assessed coronary plaque vulnerability or CAC score. Conclusions: In patients with non-ST-segment elevation acute coronary syndrome (NSTE-ACS), ^{18}F-FDG uptake in the DA was associated with a low level of serum CysC. There was no relation between CysC levels and OCT-assessed coronary plaque vulnerability or CAC score. These findings suggest that high levels of CysC may not be considered as independent markers of atherosclerosis.

Keywords: cystatin C; ^{18}F-fluorodeoxyglucose-positron emission tomography; frequency domain-optical coherence tomography; coronary artery calcium score; non-ST-segment elevation acute coronary syndrome

1. Introduction

Cystatin C, a 13-kDa protein, is a member of a family of competitive inhibitors of lysosomal cysteine proteases synthesized in all nucleated cells at a constant rate [1]. Because of its small free filtration in the glomerulus, its complete reabsorption in the proximal tubule, and lack of tubular secretion, it has been proposed as a more reliable marker of renal function than serum creatinine [2,3]. Cystatin C has also emerged as a marker of cardiovascular risk since high levels of circulating cystatin C have been shown to be consistently and strongly associated with cardiovascular outcomes, in different clinical scenarios [4,5]. However, the mechanisms linking increased cystatin C levels and impaired cardiovascular outcome are not completely understood, so far, although renal dysfunction is a definite plausible link. Early studies suggested that raised cystatin C levels identify a 'preclinical' kidney dysfunction that may be associated with adverse clinical outcomes [6]. Most recently, Shlipak et al. [7], in a large meta-analysis of 11 general-population studies and 5 studies with subjects suffering from chronic renal disease, showed that use of cystatin C for estimation of the glomerular filtration rate (eGRF) improved the role of renal function in risk classification with reference to all-cause mortality, cardiovascular mortality, and renal failure. On the other hand, since elastolytic cysteine proteases and their inhibitors are involved in the pathogenesis of atherosclerosis, it has also been suggested that cystatin C levels may be directly linked to the development and progression of atherosclerosis [8,9]. However, mendelian randomization studies [10,11] have shown that the association between cystatin C and cardiovascular disease is not causal. Nonetheless, its role as a marker of atherosclerosis (reverse causality) is still controversial. Therefore, we designed the present study enrolling patients with first non-ST-segment elevation acute coronary syndrome (NSTE-ACS) to evaluate the relationship between serum cystatin C levels and different features of atherosclerosis, namely, 1) characteristics of coronary plaque vulnerability as assessed by optical coherence tomography (OCT), 2) coronary artery calcium (CAC) by means of computed tomography (CT) scan, and 3) aortic wall inflammation as assessed by ^{18}F-Fluorodeoxyglucose (^{18}F-FDG)-positron emission tomography (PET).

2. Materials and Methods

The present study is a pre-specified subanalysis of a study aimed at evaluating the relationship between aortic inflammation as assessed using ^{18}F-FDG-PET and features of coronary plaque vulnerability as assessed using OCT [12]. Briefly, we prospectively enrolled consecutive patients with NSTE-ACS referred to the S. Orsola/Malpighi Hospital Catheterization Laboratory and scheduled for percutaneous coronary intervention (PCI) for at least 1 coronary obstruction in one of the main three epicardial vessels. Inclusion and exclusion criteria have been previously described in detail [12]. Of note, although diabetes mellitus is one of the major cardiovascular risk factors, it was included in the exclusion criteria since it is known that high levels of prescan glucose value reduce aortic ^{18}F-FDG uptake and increase blood pool activity [13]. In addition to the evaluation of routine hematological and biochemical profiles, for the purpose of this sub-study an additional tube was drawn for the determination of serum Cystatin C. Serum levels of C-reactive protein (CRP) were measured using the immunoturbidimetric method [14] (AU 5800, Beckman Coulter, Brea, California, United States). Intra- and inter-individual coefficients of variation were 3.22% and 3.79%, respectively. Serum levels of cystatin C were measured using the nephelometric method [15] (Image 800, Beckman Coulter, Brea, California, United States). Intra- and inter-individual coefficients of variation ranged from 1.6% to 1.8% and 2.3% to 2.9%, respectively.

Coronary angiography and angioplasty was performed either via the trans-radial or the trans-femoral approach with the use of a 6F sheath [16]. Standard techniques and medications were used. Three vessel OCT acquisition and analyses were previously described [12,17,18]. For each patient the number of lipid-rich plaques and lipid-rich plaques with macrophages and thin cap fibroatheromas (TCFAs) were established.

All patients underwent ^{18}F-FDG-PET/Computed tomography (CT) >24 h after successful PCI procedure and before discharge. Patients preparation and ^{18}F-FDG-PET/CT protocol were previously

described [12]. ^{18}F-FDG uptake was measured within the wall of both the ascending aorta (AA) and thoracic descending aorta (DA). Superior vena cava was used to calculate the blood pool background SUV with a 1 cm standard region of interest. SUV values (maximum and mean) were calculated on an axial plane slice by slice (every 3.75 mm) around the wall of both the AA and DA. For each aortic slice, the mean and maximum target to background ratio (TBR_{mean} and TBR_{max}, respectively) was calculated by dividing the SUV_{mean} and SUV_{max} of the aorta with the SUV_{mean} of the superior vena cava. Subsequently, TBR_{mean} and TBR_{max} were averaged for both the AA and DA [19]. We also calculated the number of active slices in both the AA and DA. ^{18}F-FDG-PET slices were defined as active if TBR_{max} was $\geq$1.6, as previously described [19].

Coronary calcification was evaluated using standardized methods as previously described [20]. Low attenuation CT scanning was performed using a tube voltage of 120 kV and 80 mA and slice thickness of 3.75 mm. Previous studies have demonstrated that CAC scores measured on CT scan images obtained from a hybrid PET-CT scanner are comparable with those obtained on a dedicated CT scanner [21]. CAC score was measured in a blind fashion by a separate investigator (F.B.) from those who performed the PET analyses.

Categorical data are expressed as proportions and continuous variables reported as medians (25th–75th percentiles). Patients were divided into low cystatin C group and high cystatin C group, on the basis of the median value of serum cystatin C. For comparisons between groups, the Fisher chi-square test and Whitney's test were used for categorical and continuous variables, respectively. Correlations between cystatin C and features of atherosclerosis modelled as continuous variables were determined using the Spearman's rank correlation test. The independent association between serum cystatin C and the different features of atherosclerosis (namely characteristics of coronary plaque vulnerability, CAC, and aortic metabolic activity) were evaluated using the high cystatin C group as dependent variable by means of univariable and multivariable logistic regression. The multivariable model included both the modified diet in renal disease-estimated glomerular filtration rate (MDRD-eGFR) and CRP as confounders. A p value <0.05 in the two-tailed tests was considered significant. All analyses were performed with STATA 14.0 software (STATA Corporation, College Station, Tex).

3. Results

Figure 1 shows the study flow chart. Among 77 patients screened, 47 were initially enrolled. Of these, 13 were excluded after angiography, 1 withdrew consent for study participation, and 2 had missing cystatin C values. Therefore, the study population comprised 31 NSTE-ACS patients treated with PCI. Three patients refused to undergo FDG-PET but still agreed to participate to the study. Baseline characteristics are shown in Table 1. The median age of the study population was 65 (55–72) years, and 26 patients (84%) were male. They had a high prevalence of classical risk factor. Ischemic changes of ECG (ST deviation or inverted T waves) were observed in 21 cases (68%). The median values of creatinine and MDRD e-GFR were 0.94 mg/dL (0.77–1.02) and 87 mL/min/1.73 m^2, respectively. The median value of cystatin C was 0.95 mg/mL (0.88–1.08). There were no differences in baseline characteristics between the two study groups, with the exception of CRP values. Indeed, patients with low level of cystatin C showed a strong trend toward an increased level of CRP (0.52 vs. 0.34 ng/L, p = 0.05).

Table 1. Baseline characteristics.

Variable	All Patients	Cystatin C < 0.95 mg/mL	Cystatin C ≥ 0.95 mg/mL	*P* Value
No. of Patients	**n = 31**	**n = 14**	**n = 17**	
Age, years, median (25th–75th)	65 (55–72)	66 (56–72)	65 (51–72)	0.84
Male gender-no. (%)	26 (84)	11 (79)	15 (88)	0.63
Risk Factors				
Hypercholesterolemia-no. (%)	19 (61)	8 (57)	11 (64)	0.72
Hypertension-no. (%)	19 (61)	9 (64)	10 (59)	1.00
Smokers-no. (%)	26 (81)	12 (86)	13 (76)	0.66
Family-history of CAD-no. (%)	7 (23)	2 (14)	5 (29)	0.41
Presenting Characteristics				
Systolic BP, mmHg, median (25th–75th)	155 (140–170)	152 (140–170)	160 (150–160)	0.89
Heart rate, pulse/min, mean ± SD	75 (64–88)	84 (75–90)	73 (64–83)	0.06
ECG changes-no. (%)	21 (68)	10 (71)	11 (65)	1.00
Hb, g/dL, median (25th–75th)	14.8 (13.9–15.6)	14.5 (13.9–15.6)	14.9 (14.3–15.6)	0.56
WBC, $*10^3/mm^3$ median (25th–75th)	8.42 (6.53–12.13)	9.54 (7.57–12.13)	7.62 (6.28–11:03)	0.17
Platelet count, $*10^3/mm^3$ median (25th–75th)	254 (209–291)	273 (244–287)	226 (192–291)	0.17
Mean platelet volume, fl median (25th–75th)	7.4 (7.2–8.3)	7.5 (7.2–10.7)	7.4 (7.2–8.0)	0.35
Creatinine, mg/dL, median (25th–75th)	0.94 (0.77–1.02)	0.9 (0.76–0.96)	0.94 (0.83–1.02)	0.26
MDRD eGRF, mL/min/1.73, median (25th–75th)	87 (81–98)	87 (81–100)	97(76–96)	0.49
Cystatin C, mg/dL median (25th–75th)	0.95 (0.88–1.08)	0.88 (0.79–0.90)	1.04 (0.98–1.22)	<0.001
Low density liprotein, mg/dL median (25th–75th)	136 (106–160)	148 (127–155)	132 (102–161)	0.52
High density liprotein, mg/dL median (25th–75th)	37 (33–46)	37 (35–39)	38 (33–47)	0.72
CRP, ng/L median (25th–75th)	0.40 (0.24–0.67)	0.52 (0.29–0.95)	0.34 (0.23–0.47)	0.05
LVEF, % median (25th–75th)	57 (50–61)	59 (48–65)	57 (61–60)	0.82
Procedure				
Multivessel disease-no. (%)	14 (45)	7 (50)	7 (41)	0.73
Multivessel treatment	12 (38)	7 (50)	5 (29)	0.28
DES-no. (%)	29 (94)	14 (100)	15 (88)	0.48

BP = blood pressure; CAD = coronary artery disease; CRP = c-reactive protein; DES = drug eluting stent; LVEF = left ventricle ejection fraction, MDRD eGRF = modified diet in renal disease estimated-glomerular filtration rate, WBC = white blood cell.

Table 2 shows that there were no differences in terms of OCT-assessed features of coronary plaque vulnerability between the two study groups. Overall, patients with low levels of cystatin C were more likely to have a higher FDG uptake in the aortic wall and CAC score. When modelled as continuous variable, cystatin C levels showed a strong trend towards an inverse relationship with the number of active slices in DA (rho = −0.35, p = 0.06). Yet, after multivariable analysis, levels of cystatin C were independently associated with FGD uptake in DA as measured by either averaged max TBR or number of active slices (Table 3). Figure 2A depicts a ^{18}F-FDG-PET/CT scan from a patient in the high cystatin group showing no significant FDG uptake in the DA (max TBR = 1.3), whilst a further ^{18}F-FDG-PET/CT scan from a patient in the low cystatin C group shows an active (max TBR = 2.0) focus of FDG uptake in the DA wall (Figure 2B). There were no active slices in the AA, in both cases. Finally, no trend was found for the association of cystatin C and CAC score. Figure 3 shows that areas of FDG uptake in the aortic wall are not related to the presence of calcification.

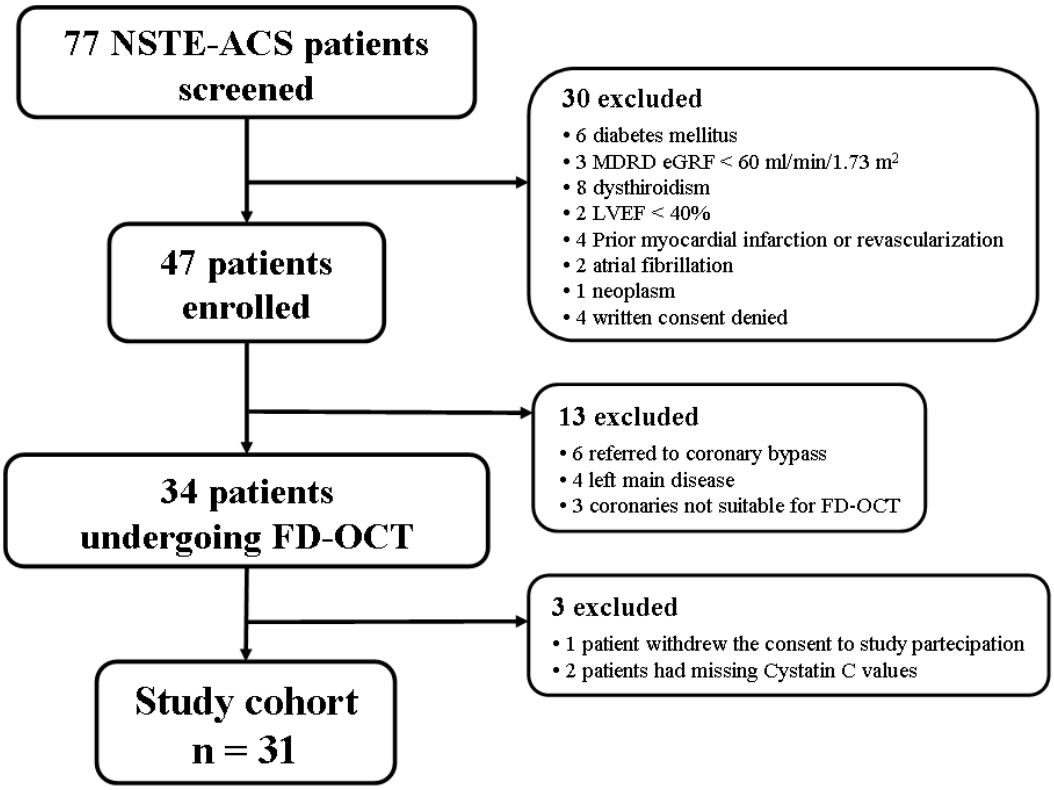

Figure 1. Study flow chart. Abbreviations: LVEF = left ventricle ejection fraction, MDRD eGRF = Modified Diet in Renal Disease estimated Glomerular Filtration Rate, ^{18}F-FDG-PET/CT = ^{18}F-Fluorodeoxyglucose-Positron Emission Tomography/Computed Tomography, FD-OCT = Frequency Domain-Optical Coherence Tomography, NSTE-ACS = Non-ST-segment Elevation-Acute Coronary Syndrome.

Table 2. Atherosclerotic features as assessed using a multimodality imaging approach according to cystatin C values.

Variable	All Patients	Cystatin C <0.95 mg/mL	Cystatin C ≥0.95 mg/mL	*P* Value
No. of Patients	**n = 31**	**n = 14 ***	**n = 17**	
Optical coherence tomography				
Lipid rich plaques, *n* median (25th–75th)	6 (4–8)	6.5 (5–8)	6 (4–7)	0.55
Lipid rich plaques with macrophages, n median (25th–75th)	2 (4–5)	4 (3–5)	4 (2–5)	0.78
TCFA, n median (25th–75th)	1 (1–2)	1 (0–3)	1 (1–3)	0.32
^{18}FDG-PET/CT				
Averaged mean TBR in AA, median (25th–75th)	1.23 (1.12–1.30)	1.24 (1.15–1.38)	1.22 (1.09–1.24)	0.23
Averaged max TBR in AA, median (25th–75th)	1.84 (1.71–2.04)	1.95 (1.80–2.21)	1.79 (1.61–1.93)	0.05
Averaged mean TBR in DA, median (25th–75th)	1.21 (1.02–1.33)	1.29 (1.11–1.41)	1.15 (0.99–1.29)	0.07
Averaged max TBR in DA, median (25th–75th)	1.74 (1.54–1.92)	1.82 (1.62–2.11)	1.61 (1.50–1.84)	0.06
Number of active slices in AA, median (25th –75th)	11.5 (9–13)	13 (11–14)	11 (9–12)	0.08
Number of active slices in DA, median (25th–75th)	22.5 (6.5–29)	25 (12–37)	18 (1–24)	0.03
CT scan				
Coronary calcium score, median (25th–75th)	955 (224–1300)	1298 (547–1339)	466 (57–1183)	0.07

AA = ascending aorta, DA = descending aorta, TBR = target to background ratio, TCFA = thin cap fibroatheroma.
* 3 patients did not undergo an ^{18}F-FDG-PET/CT scan.

Table 3. Relation between atherosclerotic features and cystatin C values. Univariable and adjusted odds ratio * for the highest cystatin C group.

Variable	Odds Ratio	95% CI	*P* Value	Adjusted Odds Ratio *	95% CI	*P* Value
Optical coherence tomography						
Lipid rich plaques, *n*	0.87	0.63–1.20	0.40	0.85	0.58–1.24	0.41
Lipid rich plaques with macrophages, *n*	1.00	0.69–1.47	0.98	0.82	0.64–1.42	0.81
TCFA, *n*	1.07	0.65–1.77	0.77	0.98	0.58–1.64	0.94
^{18}FDG-PET/CT						
Averaged mean TBR in A,	0.31	0.03–0.62	0.35	0.07	0.0003–14.8	0.33
Averaged max TBR in AA,	0.19	0.002–13.7	0.45	0.19	0.01–3.4	0.26
Averaged mean TBR in DA,	0.017	0.0002–1.49	0.07	0.02	0.00002–1.06	0.053
Averaged max TBR in DA,	0.07	0.004–1.50	0.09	0.02	0.0004–0.89	0.044
Number of active slices in AA,	0.77	0.57–1.06	0.11	0.69	0.47–1.02	0.069
Number of active slices in DA,	0.93	0.87–1.002	0.060	0.89	0.82–0.98	0.025
CT scan						
Coronary calcium score,	0.99	0.99–1.00	0.50	0.99	0.99–1.00	0.39

AA = ascending aorta, DA = descending aorta, TBR = target to background ratio, TCFA = thin cap fibroatheroma.
* Adjusted for the C reactive protein and the Modified Diet in Renal Disease estimated Glomerular Filtration Rate.

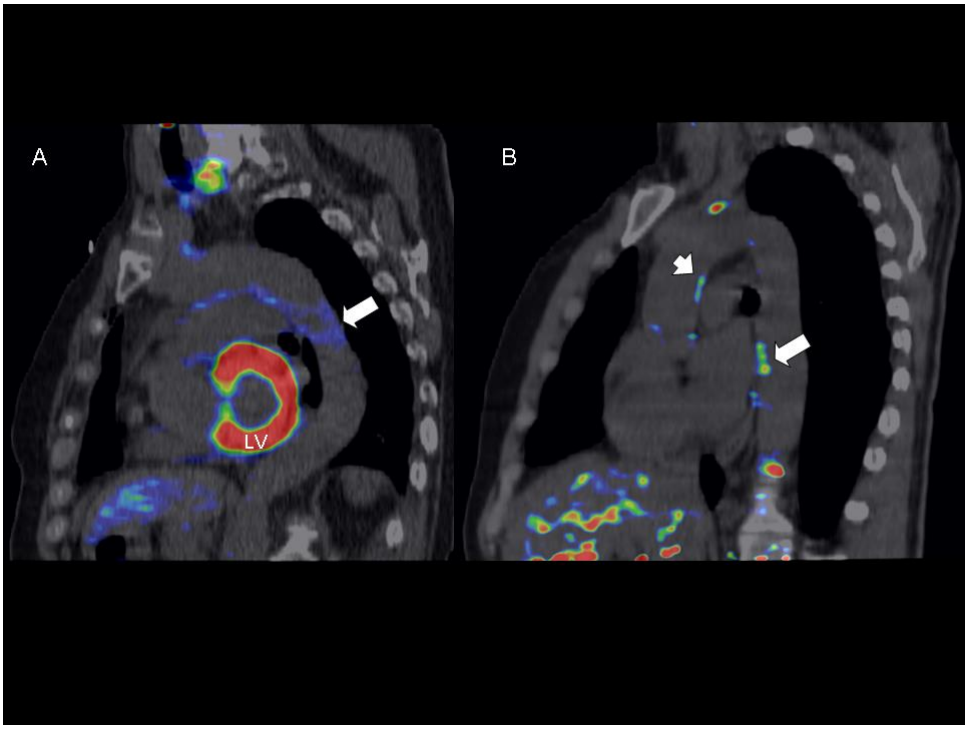

Figure 2. Representative ^{18}F-FDG-PET/CT image of thoracic aorta. (**A**) ^{18}F-FDG-PET/CT image from a patient in the high cystatin C group (cystatin C = 1.38 mg/mL) showing a non-significant focus (*arrow*) of ^{18}F-FDG uptake in the descending aortic wall with a TBR_{max} of 1.3 (^{18}F-FDG-PET slices are defined as active if TBR_{max} is $\geq$1.6) (**B**) ^{18}F-FDG-PET/CT image from a patient in the low cystatin C group (cystatin C = 0.84 mg/mL) showing an active focus of ^{18}F-FDG uptake in the descending aorta with a TBR_{max} of 2.0 (*arrow*) and a non-active focal ^{18}F-FDG uptake (*arrowhead*; TBR_{max} = 1.5) in the ascending aorta. Abbreviations: ^{18}F-FDG-PET/CT = ^{18}F-fluorodeoxyglucose-positron emission tomography/computed tomography; LV = left ventricle; TBR = target to background ratio.

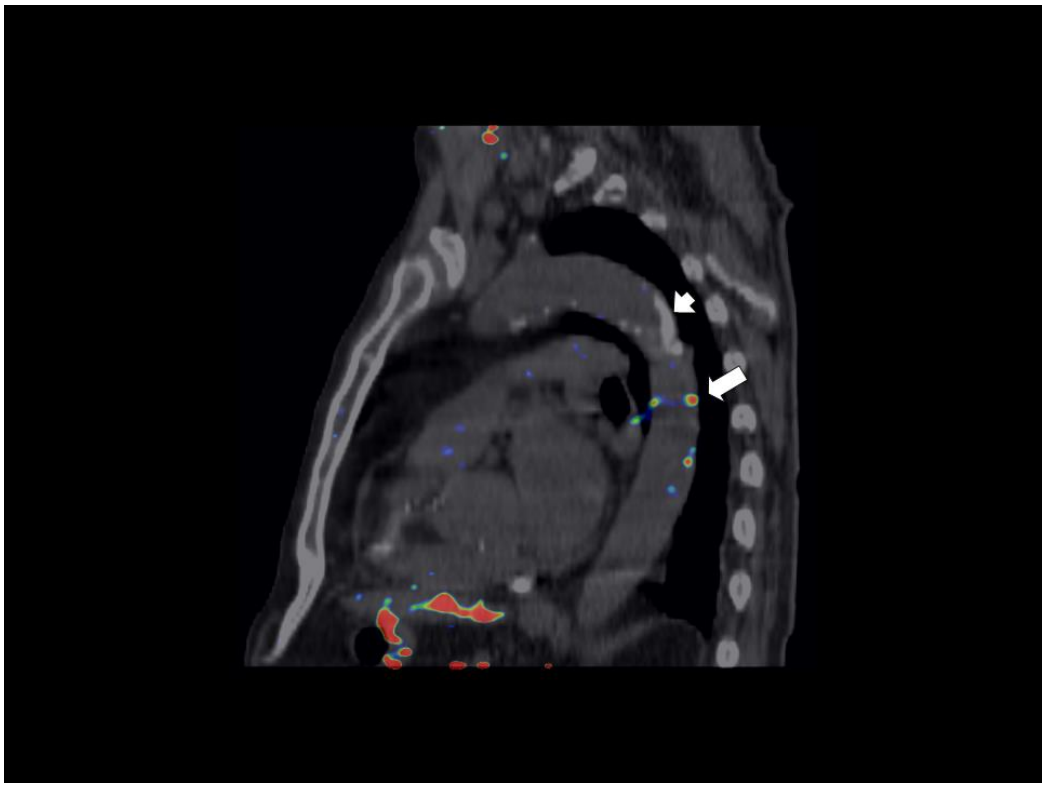

Figure 3. Representative ^{18}F-FDG-PET/CT image of thoracic aorta showing a big focal calcification (*arrowhead*) not related to significant ^{18}F-FDG uptake (TBR_{max} = 1.3). In the descending aorta, an active focal ^{18}F-FDG uptake (*arrow*) is also shown (TBR_{max} = 1.8). Abbreviations: ^{18}F-FDG-PET/CT = ^{18}F-fluorodeoxyglucose-positron emission tomography/computed tomography; TBR = target to background ratio.

4. Discussion

The main findings of the present study enrolling 31 patients with first NSTE-ACS undergoing PCI are as follows: 1) thoracic DA inflammation as assessed using ^{18}F-FDG-PET/CT and expressed in terms of TBR was independently associated with low levels of serum cystatin C; 2) there was no relationship between cystatin C levels and either features of coronary plaque vulnerability as assessed using OCT or CAC score as assessed using a CT scan.

During the past decade, cystatin C, a 13-kDa protein and member of a family of competitive inhibitors of lysosomal cysteine proteases, has gained great popularity because it has been consistently shown to be a more reliable marker of renal function than creatinine [2,3]. Yet, high levels of cystatin C have been associated with an adverse cardiovascular outcome in several observational studies involving patients with a broad spectrum of clinical conditions [4,5]. These findings, along with the observation that elastolytic cysteine proteases and their inhibitors, in particular cystatin C, are involved in the pathogenesis of atherosclerosis [8,9], have led many researchers to thoroughly investigate the link between high levels of cystatin C and impaired cardiovascular outcome. At least partially, some studies have recently shed light on this topic. First, based on the fact that several single nucleotide polymorphisms are associated with circulating cystatin C level [22,23], prospective observational studies [24,25] and mendelian randomization studies [10,11] have shown that high levels of cystatin C are not causally related to the incidence of coronary artery disease, ischemic stroke, and heart failure. In particular, mendelian randomization studies rely on a very large sample size and on the fact that genetic information, randomly distributed from parents to offspring, are not influenced by either disease status (reverse causality) or potential confounders. Secondly, it has been demonstrated that cystatin C is a more reliable marker of renal function than creatinine. It is

able to detect a small reduction in renal function that may promote atherosclerosis and an adverse outcome [7]. However, whether high levels of cystatin C are independently related to the burden of atherosclerosis (reverse causality) is, on the contrary, still controversial, with some clinical studies using angiography showing a direct [26] relationship with the extent of coronary disease and others an inverse relationship [27]. In the present study, we used a multi-imaging approach to test in vivo the relationship between serum levels of cystatin C and different features of atherosclerosis in patients with NSTE-ACS and nearly normal renal function. First, FD-OCT is a recently developed optical imaging invasive technique that provides high-resolution and cross-sectional images of coronary tissue in situ [28]. The resolution of FD-OCT (about 10 µm) is appropriate for measuring cap thickness and even plaque macrophage density. We showed that serum levels of cystatin C are not related to features of coronary plaque vulnerability, namely the number of lipid-rich plaques, lipid-rich plaques with macrophages, and TCFAs. Secondly, micro- and macro-calcification are a cardinal characteristic of atherosclerotic plaques and a hallmark of the inflammatory process [29]. CAC scoring by Agatston et al. [20] is associated with the extent of coronary plaque burden [30] and in clinical practice is considered a reliable marker of cardiovascular risk [31]. In the present study, although patients with low levels of cystatin C showed a lower median value of CAC score, we did not find any statistically significant association after univariable and multivariable analysis. These findings contrast with those observed by Imai et al. [32] who found a positive correlation between Agatston score and cystatin C levels in 410 stable patients. These discrepancies may be related to both different clinical setting and different sample size. Thirdly, unlike the previous imagine techniques that provide just morphological information, ^{18}F-FDG-PET is a molecular noninvasive imaging technique that reports on the metabolic activity of atherosclerosis since glucose is the major substrate for macrophages resident in plaque [33]. ^{18}F-FDG uptake in macrophages is positively correlated with the level of pro-inflammatory activation [34]. Accordingly, the relationship between arterial ^{18}F-FDG signal and plaque macrophage infiltration has been reported both in animal models [35] and humans, especially at the level of carotid plaques, aorta, and iliac-femoral arteries [36–38]. In the present study, we found that ^{18}F-FDG uptake in the thoracic DA was associated with low levels of serum cystatin C after adjustment for CRP and eGRF. This association was not observed for the ^{18}F-FDG uptake in the AA wall suggesting that the presence of atherosclerotic plaques increases substantially from the ascending aorta to the descending aorta [39]. Therefore, findings of the present study support in vivo data obtained from experimental studies showing that macrophage activation in atherosclerotic lesions is associated with an increased level of elastolytic cathepsins and decreased level of their inhibitors, such as cystatin C [40,41]. Notably, our study had several exclusion criteria aimed at excluding cardiac and non-cardiac conditions that may be associated with either secondary forms of acute coronary syndrome or release of pro-inflammatory mediators. In particular, patients with heart failure [42], corticoid treatment [43], and thyroid dysfunction [44] that may have influenced circulating cystatin C levels were excluded. Taken together, the findings of our study do not support the theory that high levels of cystatin C are independently associated with the extent of coronary disease. On the contrary, we showed that metabolic plaque activity in the DA wall was associated with low levels of serum cystatin C. Given these observations and the available literature, we suggest that high levels of cystatin C represent mainly a marker of renal function abnormalities that promote impaired outcome, rather than a marker of atherosclerosis.

The results of the present study should be interpreted with caution in light of some limitations. Since no data were available regarding the relationship between FDG uptake in the aortic wall and serum cystatin C levels we were prevented from calculating the sample size a priori. Nonetheless, we found a statistically significant association between FDG uptake in the DA and cystatin C levels. However, this finding showed a certain degree of imprecision with wide confidence intervals. As mentioned above, owing to our small sample size we could have missed some significant relationship as well.

Although the 2 study groups were well balanced in terms of baseline characteristics, the effect of unknown confounders on cystatin C values cannot be ruled out. In particular, we do not know the distribution of genetic polymorphisms in the study population.

Because of several technical issues such as ^{18}F-FDG -PET low spatial resolution, small size of coronary plaques, cardiac motion, and myocardium avidity for glucose as energetic substrate, using ^{18}F-FDG-PET to measure inflammation in coronary artery plaques is suboptimal [45]. Conversely, ^{18}F-sodium fluoride [45] has been shown to better identify coronary plaques with high-risk features, but this was beyond the scope of our study. However, it has been extensively demonstrated that ^{18}F-FDG activity in the great artery wall such as the aorta or the carotid arteries correlates with macrophage infiltration along with other features of plaque vulnerability [38,46,47], is highly reproducible [48], and predicts outcome [49]. These characteristics have led to an increasing use of ^{18}F-FDG-PET as surrogate endpoint in trials of novel therapies endpoint [50] and makes this tool particularly suitable for studies like ours aimed at exploring the association between an imputed biomarker of atherosclerosis and the metabolic activity within the atheroma. Nonetheless, the utilization of other PET tracer such as ^{18}F-sodium fluoride would allow the evaluation of the association between biomarkers and intimal micro-calcification that have also been associated with plaque vulnerability and progression [51]. Yet, dual-tracer ^{18}F-FDG-^{18}F-sodium fluoride PET/Magnetic Resonance [52] or CT [53] have been suggested for in vivo simultaneous clinical evaluation of both inflammation and micro-calcification that might increase understanding of mechanisms of atherosclerosis.

5. Conclusions

In patients with first NSTEACS, ^{18}F-FDG uptake in the DA was independently associated with a low level of serum cystatin C. There was no relationship between cystatin C levels and features of coronary plaque vulnerability as assessed using OCT or CAC score as assessed using CT scan. These findings suggest that high levels of CysC may not be considered as independent markers of atherosclerosis.

Author Contributions: Conceived and designed the experiments: N.T., C.N. Data acquisition: N.T., F.S., G.G., C.N., A.G.B. Analyzed the data: F.B., R.B., G.M.L., V.M., F.P. Drafting and revision of the paper: N.T., F.S., F.P., S.F., C.R.

Acknowledgments: This work was supported by the Department of Experimental, Diagnostic and Specialty Medicine—DIMES, University of Bologna and by Fanti Melloni Foundation (grant number = not applicable).

Conflicts of Interest: F.P. is a consultant for St. Jude Medical. The remaining authors have no conflicts of interest to declare.

References

1. Abrahamson, M.; Dalboge, H.; Olafsson, I.; Carlsen, S.; Grubb, A. Efficient production of native, biologically active human cystatin C by Escherichia coli. *FEBS Lett.* **1988**, *236*, 14–18. [CrossRef]
2. Dharnidharka, V.R.; Kwon, C.; Stevens, G. Serum cystatin C is superior to serum creatinine as a marker of kidney function: A meta-analysis. *Am. J. Kidney Dis.* **2002**, *40*, 221–226. [CrossRef] [PubMed]
3. Grubb, A.; Nyman, U.; Björk, J.; Lindström, V.; Rippe, B.; Sterner, G.; Christensson, A. Simple cystatin C-based prediction equations for glomerular filtration rate compared with the modification of diet in renal disease prediction equation for adults and the Schwartz and the Counahan-Barratt prediction equations for children. *Clin. Chem.* **2005**, *51*, 1420–1431. [CrossRef] [PubMed]
4. Lee, M.; Saver, J.L.; Huang, W.H.; Chow, J.; Chang, K.H.; Ovbiagele, B. Impact of elevated cystatin C level on cardiovascular disease risk in predominantly high cardiovascular risk populations: A meta-analysis. *Circ. Cardiovasc. Qual. Outcomes* **2010**, *3*, 675–683. [CrossRef]
5. Taglieri, N.; Koenig, W.; Kaski, J.C. Cystatin C and cardiovascular risk. *Clin. Chem.* **2009**, *55*, 1932–1943. [CrossRef] [PubMed]

6. Shlipak, M.G.; Katz, R.; Sarnak, M.J.; Fried, L.F.; Newman, A.B.; Stehman-Breen, C.; Seliger, S.L.; Kestenbaum, B.; Psaty, B.; Tracy, R.P.; et al. Cystatin C and prognosis for cardiovascular and kidney outcomes in elderly persons without chronic kidney disease. *Ann. Intern. Med.* **2006**, *145*, 237–246. [CrossRef] [PubMed]
7. Shlipak, M.G.; Matsushita, K.; Ärnlöv, J.; Inker, L.A.; Katz, R.; Polkinghorne, K.R.; Rothenbacher, D.; Sarnak, M.J.; Astor, B.C.; Coresh, J.; et al. Cystatin C versus creatinine in determining risk based on kidney function. *N. Engl. J. Med.* **2013**, *369*, 932–943. [CrossRef]
8. Liu, J.; Sukhova, G.K.; Sun, J.S.; Xu, W.H.; Libby, P.; Shi, G.P. Lysosomal cysteine proteases in atherosclerosis. *Arter. Thromb. Vasc. Biol.* **2004**, *24*, 1359–1366. [CrossRef]
9. Shi, G.P.; Sukhova, G.K.; Grubb, A.; Ducharme, A.; Rhode, L.H.; Lee, R.T.; Ridker, P.M.; Libby, P.; Chapman, H.A. Cystatin C deficiency in human atherosclerosis and aortic aneurysms. *J. Clin. Investig.* **1999**, *104*, 1191–1197. [CrossRef]
10. Svensson-Färbom, P.; Almgren, P.; Hedblad, B.; Engström, G.; Persson, M.; Christensson, A.; Melander, O. Cystatin C Is Not Causally Related to Coronary Artery Disease. *PLoS ONE* **2015**, *10*, e0129269. [CrossRef]
11. Van Der Laan, S.W.; Fall, T.; Soumaré, A.; Teumer, A.; Sedaghat, S.; Baumert, J.; Zabaneh, D.; van Setten, J.; Isgum, I.; Galesloot, T.E.; et al. Cystatin C and Cardiovascular Disease: A Mendelian Randomization Study. *J. Am. Coll. Cardiol.* **2016**, *68*, 934–945. [CrossRef] [PubMed]
12. Taglieri, N.; Nanni, C.; Ghetti, G.; Bonfiglioli, R.; Saia, F.; Bacchi Reggiani, M.L.; Lima, G.M.; Marco, V.; Prati, F.; Fanti, S.; et al. Relation between thoracic aortic inflammation and features of plaque vulnerability in the coronary tree in patients with non-ST-segment elevation acute coronary syndrome undergoing percutaneous coronary intervention. An FDG-positron emission tomography and optical coherence tomography study. *Eur. J. Nucl. Med. Mol. Imaging* **2017**, *44*, 1878–1887.
13. Bucerius, J.; Mani, V.; Moncrieff, C.; Machac, J.; Fuster, V.; Farkouh, M.E.; Tawakol, A.; Rudd, J.H.; Fayad, Z.A. Optimizing ^{18}F-FDG PET/CT imaging of vessel wall inflammation: The impact of ^{18}F-FDG circulation time, injected dose, uptake parameters, and fasting blood glucose levels. *Eur. J. Nucl. Med. Mol. Imaging* **2014**, *41*, 369–383. [CrossRef]
14. Borque, L.; Bellod, L.; Rus, A.; Seco, M.L.; Galisteo-Gonzalez, F. Development and validation of an automated and ultrasensitive immunoturbidimetric assay for C-reactive protein. *Clin. Chem.* **2000**, *46*, 1839–1842. [PubMed]
15. Mussap, M.; Ruzzante, N.; Varagnolo, M.; Plebani, M. Quantitative automated particle-enhanced immunonephelometric assay for the routinary measurement of human cystatin C. *Clin. Chem. Lab. Med.* **1998**, *36*, 859–865. [CrossRef] [PubMed]
16. Bashore, T.M.; Bates, E.R.; Berger, P.B.; Clark, D.A.; Cusma, J.T.; Dehmer, G.J.; Kern, M.J.; Laskey, W.K.; O'Laughlin, M.P.; Oesterle, S.; et al. American College of Cardiology/Society for Cardiac Angiography and Interventions Clinical Expert Consensus Document on cardiac catheterization laboratory standards. A report of the American College of Cardiology Task Force on Clinical Expert Consensus Documents. *J. Am. Coll. Cardiol.* **2001**, *37*, 2170–2214. [PubMed]
17. Di Vito, L.; Agozzino, M.; Marco, V.; Ricciardi, A.; Concardi, M.; Romagnoli, E.; Gatto, L.; Calogero, G.; Tavazzi, L.; Arbustini, E.; et al. Identification and quantification of macrophage presence in coronary atherosclerotic plaques by optical coherence tomography. *Eur. Heart. J. Cardiovasc. Imaging* **2015**, *16*, 807–813. [CrossRef] [PubMed]
18. Otsuka, F.; Joner, M.; Prati, F.; Virmani, R.; Narula, J. Clinical classification of plaque morphology in coronary disease. *Nat. Rev. Cardiol.* **2014**, *11*, 379–389. [CrossRef] [PubMed]
19. Bucerius, J.; Hyafil, F.; Verberne, H.J.; Slart, R.H.; Lindner, O.; Sciagra, R.; Agostini, D.; Ubleis, C.; Gimelli, A.; Hacker, M. Position paper of the Cardiovascular Committee of the European Association of Nuclear Medicine (EANM) on PET imaging of atherosclerosis. *Eur. J. Nucl. Med. Mol. Imaging* **2016**, *43*, 780–792. [CrossRef]
20. Agatston, A.S.; Janowitz, W.R.; Hildner, F.J.; Zusmer, N.R.; Viamonte, M., Jr.; Detrano, R. Quantification of coronary artery calcium using ultrafast computed tomography. *J. Am. Coll. Cardiol.* **1990**, *15*, 827–832. [CrossRef]
21. Einstein, A.J.; Johnson, L.L.; Bokhari, S.; Son, J.; Thompson, R.C.; Bateman, T.M.; Hayes, S.W.; Berman, D.S. Agreement of visual estimation of coronary artery calcium from low-dose CT attenuation correction scans in hybrid PET/CT and SPECT/CT with standard Agatston score. *J. Am. Coll. Cardiol.* **2010**, *56*, 1914–1921. [CrossRef]

22. Chambers, J.C.; Zhang, W.; Lord, G.M.; van der Harst, P.; Lawlor, D.A.; Sehmi, J.S.; Gale, D.P.; Wass, M.N.; Ahmadi, K.R.; Bakker, S.J.; et al. Genetic loci influencing kidney function and chronic kidney disease. *Nat. Genet.* **2010**, *42*, 373–375. [CrossRef] [PubMed]
23. Kottgen, A.; Pattaro, C.; Boger, C.A.; Fuchsberger, C.; Olden, M.; Glazer, N.L.; Parsa, A.; Gao, X.; Yang, Q.; Smith, A.V.; et al. New loci associated with kidney function and chronic kidney disease. *Nat. Genet.* **2010**, *42*, 376–384. [CrossRef] [PubMed]
24. Akerblom, A.; Eriksson, N.; Wallentin, L.; Siegbahn, A.; Barratt, B.J.; Becker, R.C.; Budaj, A.; Himmelmann, A.; Husted, S.; Storey, R.F.; et al. Polymorphism of the cystatin C gene in patients with acute coronary syndromes: Results from the PLATelet inhibition and patient Outcomes study. *Am. Heart J.* **2014**, *168*, 96–102.e2. [CrossRef]
25. Loew, M.; Hoffmann, M.M.; Koenig, W.; Brenner, H.; Rothenbacher, D. Genotype and plasma concentration of cystatin C in patients with coronary heart disease and risk for secondary cardiovascular events. *Arter. Thromb. Vasc. Biol.* **2005**, *25*, 1470–1474. [CrossRef] [PubMed]
26. Niccoli, G.; Conte, M.; Della Bona, R.; Altamura, L.; Siviglia, M.; Dato, I.; Ferrante, G.; Leone, A.M.; Porto, I.; Burzotta, F.; et al. Cystatin C is associated with an increased coronary atherosclerotic burden and a stable plaque phenotype in patients with ischemic heart disease and normal glomerular filtration rate. *Atherosclerosis* **2008**, *198*, 373–380. [CrossRef] [PubMed]
27. Doganer, Y.C.; Aydogan, U.; Aydogdu, A.; Aparci, M.; Akbulut, H.; Nerkiz, P.; Turker, T.; Cayci, T.; Barcin, C.; Saglam, K. Relationship of cystatin C with coronary artery disease and its severity. *Coronary Artery Dis.* **2013**, *24*, 119–126. [CrossRef]
28. Prati, F.; Regar, E.; Mintz, G.S.; Arbustini, E.; Di Mario, C.; Jang, I.K.; Akasaka, T.; Costa, M.; Guagliumi, G.; Grube, E.; et al. Expert review document on methodology, terminology, and clinical applications of optical coherence tomography: Physical principles, methodology of image acquisition, and clinical application for assessment of coronary arteries and atherosclerosis. *Eur. Heart J.* **2010**, *31*, 401–415. [CrossRef]
29. Huang, H.; Virmani, R.; Younis, H.; Burke, A.P.; Kamm, R.D.; Lee, R.T. The impact of calcification on the biomechanical stability of atherosclerotic plaques. *Circulation* **2001**, *103*, 1051–1056. [CrossRef]
30. Sangiorgi, G.; Rumberger, J.A.; Severson, A.; Edwards, W.D.; Gregoire, J.; Fitzpatrick, L.A.; Schwartz, R.S. Arterial calcification and not lumen stenosis is highly correlated with atherosclerotic plaque burden in humans: A histologic study of 723 coronary artery segments using nondecalcifying methodology. *J. Am. Coll. Cardiol.* **1998**, *31*, 126–133. [CrossRef]
31. Greenland, P.; Alpert, J.S.; Beller, G.A.; Benjamin, E.J.; Budoff, M.J.; Fayad, Z.A.; Foster, E.; Hlatky, M.A.; Hodgson, J.M.; Kushner, F.G.; et al. 2010 ACCF/AHA guideline for assessment of cardiovascular risk in asymptomatic adults: A report of the American College of Cardiology Foundation/American Heart Association Task Force on Practice Guidelines. *Circulation* **2010**, *122*, e584–e636. [PubMed]
32. Imai, A.; Komatsu, S.; Ohara, T.; Kamata, T.; Yoshida, J.; Miyaji, K.; Shimizu, Y.; Takewa, M.; Hirayama, A.; Deshpande, G.A.; et al. Serum cystatin C is associated with early stage coronary atherosclerotic plaque morphology on multidetector computed tomography. *Atherosclerosis* **2011**, *218*, 350–355. [CrossRef] [PubMed]
33. Joseph, P.; Tawakol, A. Imaging atherosclerosis with positron emission tomography. *Eur. Heart J.* **2016**, *37*, 2974–2980. [CrossRef] [PubMed]
34. Tawakol, A.; Singh, P.; Mojena, M.; Pimentel-Santillana, M.; Emami, H.; MacNabb, M.; Rudd, J.H.; Narula, J.; Enriquez, J.A.; Traves, P.G.; et al. HIF-1alpha and PFKFB3 Mediate a Tight Relationship Between Proinflammatory Activation and Anerobic Metabolism in Atherosclerotic Macrophages. *Arter. Thromb. Vasc. Biol.* **2015**, *35*, 1463–1471. [CrossRef] [PubMed]
35. Aziz, K.; Berger, K.; Claycombe, K.; Huang, R.; Patel, R.; Abela, G.S. Noninvasive detection and localization of vulnerable plaque and arterial thrombosis with computed tomography angiography/positron emission tomography. *Circulation* **2008**, *117*, 2061–2070. [CrossRef] [PubMed]
36. Rudd, J.H.; Myers, K.S.; Bansilal, S.S.; Machac, J.; Woodward, M.; Fuster, V.; Farkouh, M.E.; Fayad, Z.A. Relationships among regional arterial inflammation, calcification, risk factors, and biomarkers: A prospective fluorodeoxyglucose positron-emission tomography/computed tomography imaging study. *Circ. Cardiovasc. Imaging* **2009**, *2*, 107–115. [CrossRef] [PubMed]
37. Tatsumi, M.; Cohade, C.; Nakamoto, Y.; Wahl, R.L. Fluorodeoxyglucose uptake in the aortic wall at PET/CT: Possible finding for active atherosclerosis. *Radiology* **2003**, *229*, 831–837. [CrossRef]

38. Tawakol, A.; Migrino, R.Q.; Bashian, G.G.; Bedri, S.; Vermylen, D.; Cury, R.C.; Yates, D.; LaMuraglia, G.M.; Furie, K.; Houser, S.; et al. In vivo ^{18}F-fluorodeoxyglucose positron emission tomography imaging provides a noninvasive measure of carotid plaque inflammation in patients. *J. Am. Coll. Cardiol.* **2006**, *48*, 1818–1824. [CrossRef]
39. Stone, J.R.; Bruneval, P.; Angelini, A.; Bartoloni, G.; Basso, C.; Batoroeva, L.; Buja, L.M.; Butany, J.; d'Amati, G.; Fallon, J.T.; et al. Consensus statement on surgical pathology of the aorta from the Society for Cardiovascular Pathology and the Association for European Cardiovascular Pathology: I. Inflammatory diseases. *Cardiovasc. Pathol.* **2015**, *24*, 267–278. [CrossRef]
40. Oorni, K.; Sneck, M.; Bromme, D.; Pentikainen, M.O.; Lindstedt, K.A.; Mayranpaa, M.; Aitio, H.; Kovanen, P.T. Cysteine protease cathepsin F is expressed in human atherosclerotic lesions, is secreted by cultured macrophages, and modifies low density lipoprotein particles in vitro. *J. Biol. Chem.* **2004**, *279*, 34776–34784. [CrossRef]
41. Schulte, S.; Sun, J.; Libby, P.; Macfarlane, L.; Sun, C.; Lopez-Ilasaca, M.; Shi, G.P.; Sukhova, G.K. Cystatin C deficiency promotes inflammation in angiotensin II-induced abdominal aortic aneurisms in atherosclerotic mice. *Am. J. Pathol.* **2010**, *177*, 456–463. [CrossRef] [PubMed]
42. Maurer, M.S.; Burkhoff, D.; Fried, L.P.; Gottdiener, J.; King, D.L.; Kitzman, D.W. Ventricular structure and function in hypertensive participants with heart failure and a normal ejection fraction: The Cardiovascular Health Study. *J. Am. Coll. Cardiol.* **2007**, *49*, 972–981. [CrossRef] [PubMed]
43. Risch, L.; Herklotz, R.; Blumberg, A.; Huber, A.R. Effects of glucocorticoid immunosuppression on serum cystatin C concentrations in renal transplant patients. *Clin. Chem.* **2001**, *47*, 2055–2059. [PubMed]
44. Manetti, L.; Pardini, E.; Genovesi, M.; Campomori, A.; Grasso, L.; Morselli, L.L.; Lupi, I.; Pellegrini, G.; Bartalena, L.; Bogazzi, F.; et al. Thyroid function differently affects serum cystatin C and creatinine concentrations. *J. Endocrinol. Investig.* **2005**, *28*, 346–349. [CrossRef]
45. Joshi, N.V.; Vesey, A.T.; Williams, M.C.; Shah, A.S.; Calvert, P.A.; Craighead, F.H.; Yeoh, S.E.; Wallace, W.; Salter, D.; Fletcher, A.M.; et al. ^{18}F-fluoride positron emission tomography for identification of ruptured and high-risk coronary atherosclerotic plaques: A prospective clinical trial. *Lancet* **2014**, *383*, 705–713. [CrossRef]
46. Figueroa, A.L.; Subramanian, S.S.; Cury, R.C.; Truong, Q.A.; Gardecki, J.A.; Tearney, G.J.; Hoffmann, U.; Brady, T.J.; Tawakol, A. Distribution of inflammation within carotid atherosclerotic plaques with high-risk morphological features: A comparison between positron emission tomography activity, plaque morphology, and histopathology. *Circ. Cardiovasc. Imaging* **2012**, *5*, 69–77. [CrossRef] [PubMed]
47. Silvera, S.S.; Aidi, H.E.; Rudd, J.H.; Mani, V.; Yang, L.; Farkouh, M.; Fuster, V.; Fayad, Z.A. Multimodality imaging of atherosclerotic plaque activity and composition using FDG-PET/CT and MRI in carotid and femoral arteries. *Atherosclerosis* **2009**, *207*, 139–143. [CrossRef]
48. Rudd, J.H.; Myers, K.S.; Bansilal, S.; Machac, J.; Rafique, A.; Farkouh, M.; Fuster, V.; Fayad, Z.A. 18 Fluorodeoxyglucose positron emission tomography imaging of atherosclerotic plaque inflammation is highly reproducible: Implications for atherosclerosis therapy trials. *J. Am. Coll. Cardiol.* **2007**, *50*, 892–896. [CrossRef]
49. Figueroa, A.L.; Abdelbaky, A.; Truong, Q.A.; Corsini, E.; MacNabb, M.H.; Lavender, Z.R.; Lawler, M.A.; Grinspoon, S.K.; Brady, T.J.; Nasir, K.; et al. Measurement of arterial activity on routine FDG PET/CT images improves prediction of risk of future CV events. *JACC Cardiovasc. Imaging* **2013**, *6*, 1250–1259. [CrossRef]
50. Tahara, N.; Kai, H.; Ishibashi, M.; Nakaura, H.; Kaida, H.; Baba, K.; Hayabuchi, N.; Imaizumi, T. Simvastatin attenuates plaque inflammation: Evaluation by fluorodeoxyglucose positron emission tomography. *J. Am. Coll. Cardiol.* **2006**, *48*, 1825–1831. [CrossRef]
51. Hutcheson, J.D.; Maldonado, N.; Aikawa, E. Small entities with large impact: Microcalcifications and atherosclerotic plaque vulnerability. *Curr. Opin. Lipidol.* **2014**, *25*, 327–332. [CrossRef] [PubMed]
52. Karakatsanis, N.; Trivieri MDweck, M.; Philip Robson, P.; Abgral, R.; Soler, R.; Calcagno, C.; Mani, V.; Tsoumpas, C.; Kovasic, J.; et al. Simultaneous assessment of carotid plaque inflammation and micro-calcification with dual-tracer ^{18}F-FDG: ^{18}F-NaF PET-MR imaging: A clinical feasibility study. *J. Nucl. Med.* **2017**, *58*, 446.
53. Li, X.; Heber, D.; Wadsak, W.; Mitterhauser, M.; Hacker, M. Combined ^{18}F-FDG PET/CT and ^{18}F-NaF PET/CT imaging in assessing vascular inflammation and osteogenesis in calcified atherosclerotic lesions. *J. Nucl. Med.* **2016**, *57*, 68.

© 2019 by the authors. Licensee MDPI, Basel, Switzerland. This article is an open access article distributed under the terms and conditions of the Creative Commons Attribution (CC BY) license (http://creativecommons.org/licenses/by/4.0/).